Structure of a DNA Repair Substrate Containing an Alkyl Interstrand Cross-Link at 1.65 Å Resolution[†,‡]

Matthew C. Swenson,[§] Shanthi R. Paranawithana,[§,||] Paul S. Miller,* and Clara L. Kielkopf*[,⊥]

Department of Biochemistry and Molecular Biology, Bloomberg School of Public Health, Johns Hopkins University, Baltimore, Maryland 21205

Received January 18, 2007; Revised Manuscript Received February 19, 2007

ABSTRACT: Chemotherapeutic alkylating agents, such as bifunctional nitrogen mustards and cisplatins, generate interstrand DNA cross-links that inhibit cell proliferation by arresting DNA transcription and replication. A synthetic N^4C-ethyl-N^4C interstrand cross-link between opposing cytidines mimics the DNA damage produced by this class of clinically important compounds and can be synthesized in large quantities to study the repair, physical properties, and structures of these DNA adducts. The X-ray structure of a DNA duplex d(CCAA**C***GTTGG)$_2$ containing a synthetic N^4C-ethyl-N^4C interstrand cross-link between the cytosines of the central CpG step (*) has been determined at 1.65 Å resolution. This structure reveals that the ethyl cross-link in the CpG major groove does not significantly disrupt the B-form DNA helix. Comparison of the N^4C-ethyl-N^4C cross-linked structure with the structure of an un-cross-linked oligonucleotide of the same sequence reveals that the cross-link selectively stabilizes a preexisting alternative conformation. The conformation preferred by the cross-linked DNA is constrained by the geometry of the ethyl group bridging the cytosine amines. Characteristics of the cross-linked CpG step include subtle differences in the roll of the base pairs, optimized Watson−Crick hydrogen bonds, and loss of a divalent cation binding site. Given that the N^4C-ethyl-N^4C cross-link stabilizes a preexisting conformation of the CpG step, this synthetically accessible substrate presents an ideal model system for studying the genomic effects of covalently coupling the DNA strands, independent of gross alterations in DNA structure.

DNA cross-linking agents, including bischloroethylnitrosoureas, cisplatins, and nitrogen mustards such as melphalan and oxazaphosphorine are widely prescribed as chemotherapeutic treatments for cancers. These chemotherapeutics exert their toxic effects by forming interstrand DNA cross-links, which block the essential processes of transcription and replication by preventing separation of the DNA strands (reviewed in refs *1* and *2*). In addition, unsolicited DNA interstrand cross-links may arise naturally from unavoidable exposure to endogenous compounds such as the products of lipid peroxidation (*3*) or environmentally derived compounds such as formaldehyde (*4*). Cells have developed a variety of mechanisms, including homologous recombination and nucleotide excision repair (NER),[1] to identify and repair interstrand DNA cross-links. Accordingly, enhanced DNA repair plays a major role in the resistance of certain cancers to chemotherapy, for example, melphalan-resistant multiple myeloma (*5*) or oxazaphosphorine-resistant medulloblastoma (*6*). Given that failed cancer treatment often results from drug resistance, a clear understanding of the molecular mechanisms involved in the recognition and repair of DNA interstrand cross-links would facilitate the development of more effective chemotherapeutic agents.

Interstrand cross-links are only a minor percentage (1−5%) of the adducts formed by most of DNA alkylating agents, although interstrand DNA cross-links are by far the most toxic (*7*, *8*) and, therefore, the most physiologically relevant adduct for investigation. The low availability of defined DNA cross-links is a roadblock to studying their structure and repair. Using an approach in which the cross-link is introduced during solid-phase DNA synthesis, short DNA duplexes containing N^4C-alkyl-N^4C interstrand cross-links have been synthesized in quantities sufficient for detailed structural and mechanistic investigation (*9*−*12*). These synthetic N^4C-alkyl-N^4C interstrand cross-links provide a well-defined mimic of the DNA damage introduced by therapeutic DNA alkylating agents.

DNA interstrand cross-links produced by different chemical agents induce a variety of structural changes in DNA (*2*). This structural diversity could lead to differences in the mechanism and effectiveness of repair and, hence, to the physiological activity of the DNA cross-linking agent. The

[†] This research was supported by a grant from the National Cancer Institute (CA082785). M.C.S. and S.R.P. were supported in part by a training grant from the National Cancer Institute (CA009110).

[‡] Atomic coordinates and structure factors are available in the RCSB Protein Data Bank (2OKS).

* To whom correspondence should be addressed. C.L.K.: phone, 585-273-4799; fax, 585-275-6007; e-mail, clara_kielkopf@urmc.rochester.edu. P.S.M.: phone, 410-955-3489; fax, 410-955-2926; e-mail, pmiller@jhsph.edu.

[§] M.C.S. and S.R.P. contributed equally to this work.

[||] Current address: Department of Chemistry, Hampton University, Hampton, VA 23668.

[⊥] Current address: Department of Biochemistry and Biophysics, University of Rochester Medical School, Rochester, NY 14642.

[1] Abbreviations: DDP, diamminedichloroplatinum; MMC, mitomycin C; NER, nucleotide excision repair; PDB, Protein Data Bank; Tris, tris(hydroxymethyl)aminomethane.

10.1021/bi700109r CCC: $37.00
Published on Web 03/22/2007

relationship between structure and repair of interstrand cross-linked DNA was investigated by studying two different orientations of the same N^4C-ethyl-N^4C interstrand cross-link, connecting cytidines in a single CpG versus GpC step of double-stranded DNA (*13*). Both cross-link orientations were repaired efficiently in wild-type and homologous-recombination deficient *Escherichia coli*. However, a functional NER pathway was required for the cross-linked CpG step to be repaired efficiently, whereas the cross-linked GpC step was repaired efficiently regardless of the status of the NER pathway. Proton chemical shifts coupled with distance-restrained molecular dynamic regularization established that the structure of a DNA duplex containing the N^4C-ethyl-N^4C cross-link at a CpG step remains undistorted. In contrast, an oligonucleotide in which the orientation of the cross-link was reversed to a GpC step behaves poorly in NMR experiments. Moreover, atomic force microscopy experiments demonstrated that longer DNAs containing the cross-linked GpC step are more flexible than the CpG counterpart. The correlated differences between the structure and repair of the two cross-link orientations suggest that undistorted DNA cross-links are recognized and repaired in a different manner from those lesions that grossly alter the overall DNA conformation.

Given the importance of correlating the structures of damaged DNAs with their mechanisms of repair, here we present a high-resolution view of an important model system for studying DNA repair, an oligonucleotide containing a synthetic N^4C-ethyl-N^4C intrastrand cross-link at a CpG step. The X-ray structure of a palindromic DNA oligonucleotide, d(CCAA**C***GTTGG)$_2$, was determined at 1.65 Å resolution (*, cross-link). Comparison with an atomic (1.0 Å) resolution structure of the un-cross-linked DNA counterpart (*14*) reveals that conformational details, which could mark the cross-linked DNA duplex for recognition by DNA repair factors, instead preexist in the unmodified structure.

MATERIALS AND METHODS

Cross-Linked DNA Synthesis and Crystallization. The DNA decamer containing the N^4C-ethyl-N^4C interstrand cross-link was synthesized, purified using strong anion-exchange HPLC, and analyzed using mass spectrometry using previously described procedures (*12*). The purified cross-linked DNA was then desalted using C-18 Sep-Pak cartridges (Waters) and dissolved in a buffer containing 22 mM ammonium acetate, 11 mM tris(hydroxymethyl)aminomethane (Tris) hydrochloride (HCl), pH 8.0, and 11 mM calcium acetate. Crystals were grown using the sitting drop vapor diffusion method at 4 °C, in which 3 μL of a reservoir solution containing 27% 2,3-methylpentadiol, 115 mM calcium acetate, and 10 mM Tris-HCl, pH 8.0, was added to an equal volume of DNA solution, and the mixture was equilibrated against 700 μL of the reservoir solution. Crystals first appeared after 2 weeks. Prior to data collection, crystals were flash-cooled to liquid nitrogen temperatures using 35% MPD as a cryoprotectant.

X-ray Data Collection and Structure Determination. X-ray data from a single crystal were collected at a wavelength of 1.54 Å using a Rigaku rotating anode generator and Raxis-IV image plate detector at the Johns Hopkins School of Medicine (Table 1). The space group and unit cell dimensions were $C2$, $a = 31.0$ Å, $b = 24.9$ Å, $c = 34.4$ Å, and $\beta = 114.5°$, with one DNA strand per asymmetric unit of the crystal. Since this crystal form was isomorphous with the un-cross-linked oligonucleotide of identical sequence (*14*), the structure was solved by difference Fourier methods starting with the coordinates of conformation "A" of the un-cross-linked counterpart (PDB code 1EN8).

Table 1: Crystallographic Data and Refinement Statistics[a]

resolution limit (Å)	20.00−1.65
redundancy	4.0
completeness (%)	96.6 (79.4)
R_{sym}[b] (%)	4.6 (4.7)
$I/\sigma(I)$	38.2 (25.8)
no. of DNA atoms	203
no. of water atoms	87
no. of calcium ions	3
RMSD bond lengths (Å)	0.01
RMSD bond angles (deg)	1.13
average temperature factor (Å^2)	14.1
R_{cryst}[c] (%)	18.2
R_{free}[c] (%)	20.8

[a] Values in parentheses are for the highest resolution shell, 1.65−1.71 Å. [b] $R_{sym} = \sum_{hkl}\sum_i|I_i - \langle I\rangle|/\sum_{hkl}\sum_i I_i$, where I_i is an intensity I for the ith measurement of a reflection with indices hkl and $\langle I\rangle$ is the weighted mean of all measurements of I. [c] $R_{cryst} = \sum_{hkl}||F_o(hkl)| - k|F_c(hkl)||/\sum_{hkl}|F_o(hkl)|$ for the working set of reflections; R_{free} is R_{cryst} for 5.3% of the reflections excluded from the refinement.

A difference Fourier electron density map revealed well-defined electron density for the two methylene carbons of the alkyl interstrand cross-link (Figure 1), which are related by the 2-fold symmetry axis of the crystal. The methylene carbon was placed manually using the program O (*15*). The topology and parameter files for the cross-linked cystosine were generated using XPLO2D of the Uppsala Software Factory and then modified manually for chemically reasonable restraints (*16*). The structure was refined using CNSsolve v.1.1 (*17*). Three water molecules were reassigned as Ca^{2+} ions based on coordination geometry and unusually low-temperature factors. Final refinement statistics are given in Table 1. The SigmaA-estimated coordinate error of the structure is 0.15 Å (*18*). Global helical parameters were calculated using the program Curves v5.1 (*19*), and figures were made using the Pymol molecular graphics system (htttp://www.pymol.org).

RESULTS

Overall Structure. The X-ray structure of the N^4C-ethyl-N^4C interstrand cross-linked DNA decamer of sequence d(CCAA**C***GTTGG)$_2$ was determined by difference Fourier analysis starting with the coordinates of the un-cross-linked DNA counterpart (*14*). The structure of the cross-linked DNA was refined to a final R_{cryst} of 18.7% and R_{free} of 20.2% at 1.65 Å resolution, including 87 water molecules and 3 Ca^{2+} ions (Table 1). Since the palindromic strands of the DNA duplex are related by crystallographic symmetry, the two halves of the DNA duplex share identical conformations (Figure 2).

Overall, the N^4C-ethyl-N^4C interstrand cross-link is accommodated in the major groove of an undistorted B-form DNA helix (Figure 2). The average twist, rise, and sugar pucker of the cross-linked duplex are 35°, 3.32 Å, and C2′-*endo*, respectively, compared with the standard B-DNA twist,

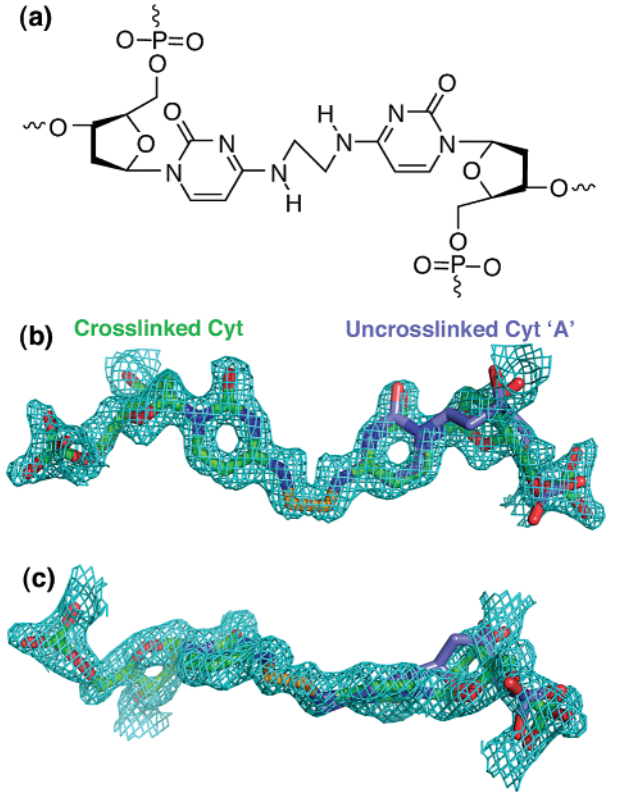

FIGURE 1: (a) Chemical structure of the N⁴C-ethyl-N⁴C cross-linked cytidines. (b) A $2|F_o| - |F_c|$ composite omit electron density map, shown at 1σ contour level around the cross-linked cytidines. For comparison, conformation A of the un-cross-linked DNA structure (colored blue) is overlaid on one of the two cross-linked cytidines (colored green), which are related by crystallographic symmetry. (c) Same as in (b) but rotated 90° about the horizontal axis.

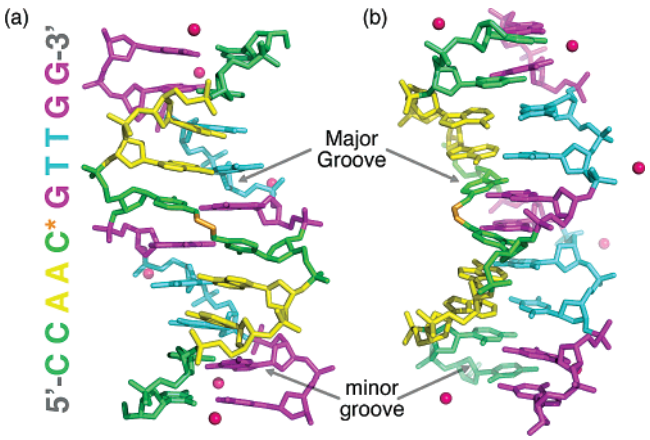

FIGURE 2: Overall X-ray structure of a DNA duplex d(CCAA**C***GTTGG)$_2$ with the N⁴C-ethyl-N⁴C interstrand cross-link between the cytosines of the central CpG step (*). Color code: Cyt, green; Thy, cyan; Gua, magenta; Ade, yellow. The ethyl cross-link is colored gold. The two strands of the double helix are related by crystallographic symmetry. The orientation in (b) is rotated 90° about the vertical axis relative to (a). The DNA sequence is shown to the left.

rise, and sugar pucker of 36°, 3.37 Å, and C3′-*exo*/C2′-*endo* (*20*). A locally overwound, helical twist (40°) at the CpG step is compensated by underwound flanking ApC and GpT steps (26°). This slight deviation from the ideal B-form prototype is unlikely to result from the N⁴C-ethyl-N⁴C interstrand cross-link, since it is shared by its un-cross-linked DNA counterpart (Table 2).

Table 2: Comparison of Helical Parameters

		un-cross-linked Cyt·Gua	
	cross-linked Cyt·Gua	minor conformation	major conformation
(a) Helical Parameters with Similarity between Cross-Linked and Un-Cross-Linked -CG- Conformations			
rise (Å)	3.4	3.5	3.5
twist (deg)	40	45	40
propeller twist (deg)	−21	3.326	3.35
buckle (deg)	3.35	3.35	3
phase (sugar pucker) (deg)	52 (C4′-*exo*)	24 (C3′-*endo*)	152 (C4′-*endo*)
shift (Å)	0.5	0.45	0.1
slide (Å)	0	0	0.5
tilt (deg)	7.0	9.8	1.8
(b) Helical Parameters with Differences between Cross-Linked and Un-Cross-Linked -CG- Conformations			
roll (deg)	12.7	−2.2	−0.2
shear (Å)	0.1	−0.3	0.2
stretch (Å)	0.0	0.5	0.2
stagger (Å)	0.0	0.2	−0.4
(c) Distances between Atoms of the Cyt·Gua Base Pair (Å)			
Cyt-N4−*Cyt-N4*	2.8	3.1	3.8
Cyt-O2−Gua-N2	2.9	3.1	3.3
Cyt-N3−Gua-N1	2.9	3.1	3.3
Cyt-N4−Gua-N6	2.9	3.0	3.3

Structure of the N⁴C-Ethyl-N⁴C Cross-Link. The exocyclic amines (N4) of the central cytosines are covalently linked by the two methylene carbons (CX) of the intervening ethyl group (Figure 3). Each of these carbons replaces one of the hydrogen atoms of the amino group, which would normally be presented in the major groove of the DNA duplex for recognition by protein molecules or interaction with solvent. On the basis of the observation of optimal hydrogen bond distances between the cytosine-N4 and guanine-O6 atoms (Table 2c), the other hydrogen atom of the amino group presumably remains undisturbed by the cross-link. Conventionally, the cytosine exocyclic amine and its attached hydrogen atoms are considered to be sp²-hybridized and coplanar with the base (*21*, *22*). However, each methylene carbon in the N⁴C-ethyl-N⁴C cross-link is slightly rotated out of the plane of the cytosine [20° from base plane, 0.45 Å shortest distance from CX to base plane calculated using Geomcalc (*23*)] (Figure 3a). This rotation allows the N4-CX−*CX-N4* torsion of the N⁴C-ethyl-N⁴C group to adopt a staggered, rather than unfavorably overlapped, conformer, with a 55° angle between N4 atoms when observed down the CX−*CX* bond (Figure 3b).

The rotation of the carbons of the ethyl cross-link out of the planes of the cytosine bases raises the possibility that the exocyclic amines are predominantly in the sp³- as opposed to the presumed sp²-hybridized state. Although the linker CX carbon and base N4 nitrogen would display similar positions if sp³-hybridized rather than sp²-hybridized, several observations suggest that the exocyclic N4 amine is at least partially sp²-hybridized. First, no hydrogen bond donors, such as bound solvent molecules or other nucleotide atoms, are observed in the vicinity of the amine. This suggests the N4 electrons are delocalized and unavailable as hydrogen bond acceptors. Second, an sp³-hybridized state of the exocyclic N4 amine would require the N4-H−C4 hydrogen bond angle (105°) to deviate by 75° from the linear ideal, notably less than the most acute angle observed in a survey of two-center hydrogen bonds (132°) (*24*). In the sp²-hybridized state, the

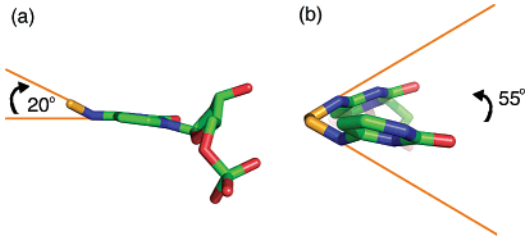

FIGURE 3: Close-up views of the cross-linked cytosines, shown as ball-and-stick diagrams and colored by atom: ethyl cross-link, gold; carbon, green; nitrogen, blue; oxygen, red. (a) Viewed along the plane of the base. (b) View in the orientation of a Newman projection, along the CX−*CX* bond.

N4−H−C4 hydrogen bond angle (160°) would deviate only 20° from linearity and would be within the most probably range of hydrogen bond angles (*24*). Thus, despite the deviation of the methylene CX carbon from the base plane, a predominately sp^2-hybridized geometry of the cytosine exocyclic amine is consistent with the observed structure and the increased thermal stability of the N^4C-ethyl-N^4C interstrand cross-linked CpG steps (*12*).

Comparison with NMR Structural Analysis. The sequence of the six nucleotides surrounding the cross-linked CpG step of the X-ray structure is identical to an N^4C-ethyl-N^4C interstrand cross-linked oligonucleotide previously studied by nuclear magnetic resonance (NMR) experiments and distance-restrained molecular dynamics [respectively d(C<u>C</u>AA**C***GTT<u>G</u>G)$_2$ and d(C<u>G</u>AA**C***GTT<u>C</u>G)$_2$, sequence differences underlined] (*13*). Although the RMSD between corresponding atoms is relatively large (2.2 Å RMSD), it is within the range of RMSDs observed for other structures determined by both NMR and X-ray crystallography (*25*). In general, the overall features of the two structures are similar, with the cross-linked CpG step embedded within an overall B-form DNA duplex. Several helical parameters of the cross-linked CpG step are shared between the X-ray and NMR structures, including a relatively large propeller twist between the bases (−21°) and a C4′-*exo* sugar pucker for the cross-linked cytidine. On the basis of the NMR structure alone, these slightly unusual helical parameters were suggested to result from the N^4C-ethyl-N^4C interstrand cross-link (*13*). However, comparison with the X-ray structure of the un-cross-linked double-stranded DNA of the same sequence, d(CCAACGTTGG)$_2$ (*14*), reveals that these characteristics are also observed in one alternative conformation of the un-cross-linked DNA, as shown in Table 2a and described below.

Similarities with the Un-Cross-Linked DNA Structure. We chose to study the DNA sequence d(CCAACGTTGG)$_2$, because the structure of this decamer has been thoroughly investigated in the un-cross-linked form (*14*, *26*). This allows the cross-linked and un-cross-linked structures to be compared to understand the influence of the N^4C-ethyl-N^4C interstrand cross-link on the DNA conformation. Two 1.0 Å resolution structures of the un-cross-linked d(CCAACGTTGG)$_2$ oligonucleotide are available, determined in the presence of either Mg^{2+} or Ca^{2+} divalent cations. Although the space group and unit cell parameters of the d(CCAACGTTGG)$_2$ structures are isomorphous, the hydration and location of bound Ca^{2+} versus Mg^{2+} counterions induce slight structural differences. In the presence of

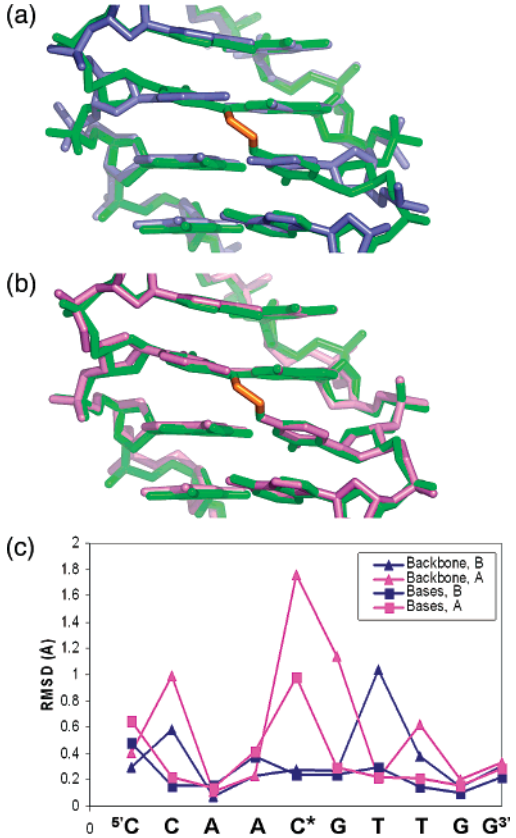

FIGURE 4: Comparison of the N^4C-ethyl-N^4C interstrand cross-linked site (green) with (a) conformation A (blue) or (b) conformation B (magenta) of the un-cross-linked structure. (c) RMSD between backbone (▲) or base atoms (■) of each nucleotide in the cross-linked structure with un-cross-linked conformation A (blue) or conformation B (magenta).

Ca^{2+} ions, the central cytidine adopts two alternative conformations of nearly equivalent occupancy, designated A and conformation "B" (*14*). In the presence of Mg^{2+} ions (*14*, *26*), a single, intermediate conformation of the cytidine is observed, consistent with previous observations that oligonucleotide structures are influenced by the type of counterion (*14*, *27*, *28*). Here, we compare the details of the N^4C-ethyl-N^4C cross-linked oligonucleotide structure, which was determined in the presence of Ca^{2+} ions, with the Ca^{2+}-containing crystal form of the un-cross-linked oligonucleotide (Figure 4).

Introducing the two-carbon linker selectively stabilizes alternative conformation B of the cytidine, with no evidence for conformation A (Figures 1 and 4). Overall, the RMSDs between all non-hydrogen atoms of the interstrand cross-linked DNA and the un-cross-linked conformations A or B are 0.5 or 0.3 Å, respectively. For comparison, the RMSD between the un-cross-linked A and B conformations is 0.5 Å, similar to the differences between the un-cross-linked conformation A and the cross-linked structure. Further inspection of the RMSDs between each nucleotide at the modified CpG step showed that the RMSDs between the cross-linked structure and the un-cross-linked conformation B are remarkably slight (0.27 and 0.24 Å for backbone or base atoms, respectively) (Figure 4c). In contrast, the largest differences between the cross-linked structure and the un-cross-linked conformation A are observed at the modified CpG step, regardless of whether backbone or base atoms

are compared (1.76 and 1.0 Å, respectively). Accordingly, a difference omit electron density map for the backbone of the cross-linked cytidine shows no trace of conformation A in the interstrand cross-linked DNA helix (Figure 1). Instead, the conformation of the interstrand cross-linked cytidine closely matched the conformation of un-cross-linked cytidine B (Figure 4b).

Comparison of the structures reveals that the *gauche* conformer of the ethyl cross-link is likely to explain the preference of the cross-linked CpG step to adopt conformation B of the un-cross-linked structure. In conformation B of the un-cross-linked structure, the exocyclic amines of the cytosines in the CpG step are 0.4 Å closer than those of conformation A. The N4 atoms of conformation B are within van der Waals contact (3.1 Å), whereas the N4 atoms of conformation A are slightly separated (3.8 Å). The observed *gauche* conformer of the N^4C-ethyl-N^4C cross-link, with the N4 atoms adjacent (Figure 3b and Table 2c), constrains the cytidines to adopt conformation B. An extended *anti* conformer would enable the N^4C-ethyl-N^4C cross-link to bridge the greater distance between the N4 atoms of conformation A. However, the *anti* conformer would drastically distort the positions of the linker CX carbons out of the planes of the cytosine bases, which would enforce predominately sp^3 hybridization on the exocyclic N4 amino group and disrupt the N4-H−O6 hydrogen bond of the base pair. Instead, the methylene carbons of the interstrand cross-link are likely to be constrained to the planes of the cytosines by delocalization of the N4 electrons.

As expected given the similarity of the cross-linked CpG site and the un-cross-linked conformation B, several helical parameters of these sites are also similar (Table 2a). In particular, the cytosines of the cross-linked base pairs and the un-cross-linked conformation B are both highly propeller twisted (−26° and −21°, respectively), which accounts for the tight packing of the exocyclic amines between the consecutive cytosines. In contrast, conformation A of the un-cross-linked CpG step has a low propeller twist (−5°), contributing to the greater distance between the cytosine exocyclic amines in the major groove. In addition, the shift, slide, and tilt parameters of the cross-linked base pair closely match those of the un-cross-linked B conformation, as opposed to the A conformation (Table 2a). The sugar puckers of both the cross-linked cytosine and the un-cross-linked B conformation are unusual, with low phase angles (52° and 24°, respectively) representative of A-form rather than B-form duplexes. Consistently, a similar, C4′-*exo* sugar pucker of the cross-linked cytosine base was also observed by NMR methods (*13*). Thus, far from distorting the DNA helix, the interstrand cross-link selectively stabilizes a preexisting alternative conformation of the d(CCAACGTTGG)$_2$ oligonucleotide.

Differences from the Un-Cross-Linked DNA Structure. Despite the many similarities between the N^4C-ethyl-N^4C cross-linked and conformation B of the un-cross-linked DNAs, a few, slight differences in the DNA conformation are evident (Table 2b). Namely, the cross-linked CpG step displays a large positive roll, which contributes to the proximity of the cytosine amines in the major groove, at the cost of opening the base pairs in the minor groove. Another notable difference is that the bases in the cross-linked pair are positioned ideally across the helical axis with no shear, stretch, or stagger, whereas the bases of the un-cross-linked conformations are slightly out of alignment. This straightening optimizes the Watson−Crick hydrogen bonds in the base pairs of the CpG step (Table 2c), which may contribute to the increased thermal stability of DNA duplexes containing the N^4C-ethyl-N^4C interstrand cross-link at the CpG step (*12*).

Comparison of Bound Calcium Ions. Four hydrated calcium ions were assigned in the un-cross-linked d(CCAACGTTGG)$_2$ structure on the basis of coordination geometry and low-temperature factors. Although the concentration of Ca^{2+} ions in the crystallization conditions of the cross-linked and un-cross-linked structures is similar (∼10 mM), only three of the four bound Ca^{2+} ions were observed in the interstrand cross-linked structure (Supporting Information, Figure S1). These three Ca^{2+} ions occupy nearly identical locations in the interstrand cross-linked structure compared with the non-cross-linked structure and are labeled consistently by numbers 111, 113, and 114. The geometry of the coordination spheres around the three Ca^{2+} ions is also preserved between the structures. Calciums 111 and 114 mediate intermolecular contacts between distinct DNA helices in the crystal lattice, and calcium 113 directly coordinates the O6 and N7 atoms in the major groove of the terminal guanines. Thus, none of the three bound Ca^{2+} ions or their coordinated water molecules directly contact the alkylated cytidine.

A fourth Ca^{2+} ion (labeled calcium 112) is bound in the minor groove of the un-cross-linked structure between the Ade•Thy base pairs and the central Cyt•Gua base pair, which would be modified by the cross-link (Figure 5). In conformation A, one water molecule from the coordination sphere of this fully hydrated Ca^{2+} ion forms a direct hydrogen bond with the deoxyribose O4′ atom of the central cytidine (2.8 Å H_2O−O4′ distance). However, the position of this water molecule is incompatible with the unusual, A-form sugar pucker of conformation B, due to steric overlap between the water oxygen and the C1′-H atoms (3.0 Å H_2O−C1′ distance, compared with 4.2 Å predicted van der Waals distance including the C1′-hydrogen with appropriate bond geometry). Hence, calcium 112 is likely to be partially occupied in the un-cross-linked structure, in a manner that is correlated with the alternative cytidine conformations.

The sugar pucker of the cross-linked cytidine is similar to that of the un-cross-linked conformation B and, accordingly, would sterically conflict with the hydrated calcium 112 (2.8 Å predicted H_2O−C1′ distance). Instead of a hydrated Ca^{2+} ion, a constellation of bound water molecules is observed in the cross-linked structure (Figure 5). Although four of these water molecules in the cross-linked structure correspond to four water ligands of calcium 112 in the un-cross-linked structure, these water molecules interact with atoms in the unmodified thymidine nucleotides rather than with the cross-linking site. No unaccounted electron density is observed near the position of calcium 112 in the un-cross-linked structure. The four bound water molecules lack the preferred coordination geometry of calcium, which ranges from six to eight ligands with calcium−oxygen ligand distances of ∼2.4 Å (*29*). Moreover, the refined temperature factors of the assigned water molecules are appropriate for oxygen (*B*-value of 19−28 Å^2 compared with *B*-values of

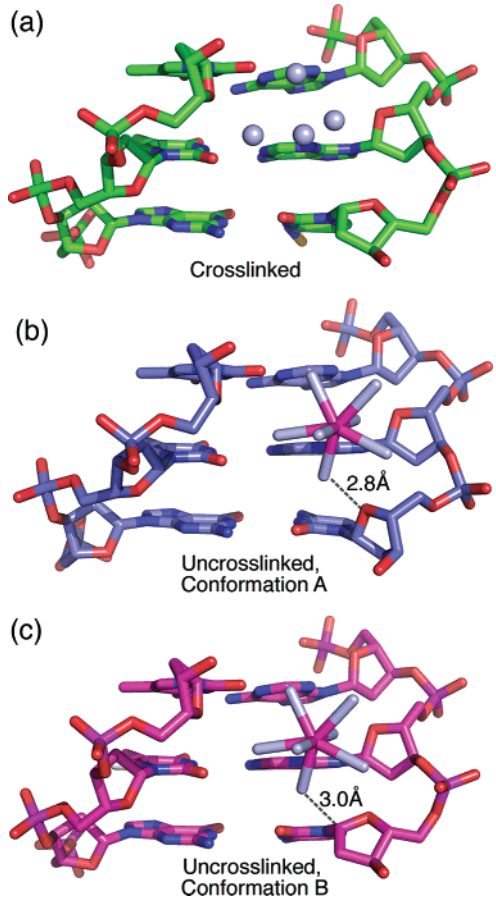

FIGURE 5: Comparison of the calcium 112 binding sites in the (a) cross-linked and (b) un-cross-linked conformation A and (c) un-cross-linked conformation B. The hydrated calcium is depicted with a ball-and-stick representation, with calcium 112 colored pink and water ligands colored light blue. The four water molecules that replace the hydrated calcium in the cross-linked structure are shown as spheres. The distances are indicated between the hydrated calcium and either the deoxyribose O4′ or C1′ atoms of conformations A or B, respectively.

1−5 Å^2 when Ca^{2+} were inappropriately assigned as H_2O). Thus, introduction of the N^{4}C-ethyl-N^{4}C interstrand cross-link eliminates a divalent cation binding site that would otherwise be presented by the un-cross-linked oligonucleotide.

DISCUSSION

Stabilized Alternative Conformations. When compared with the structure of an un-cross-linked DNA oligonucleotide of the same sequence, the synthetic N^{4}C-ethyl-N^{4}C interstrand cross-link at the CpG step does not distort the B-form DNA helix but instead fully adopts one alternative conformation of the undamaged DNA. Similarly, preexisting alternative conformations of proteins are often stabilized during RNA recognition (*30*, *31*). In particular, association with RNA selectively stabilizes a subset of alternative conformations displayed on the RNA interaction surface of the unliganded protein [hnRNP A1 (*30*) or U2AF^{65} (*31*)]. This work provides complementary evidence that alternative conformations observed in X-ray structures often play important biological roles in chemical modification and ligand binding and should not be overlooked.

Conformation of the Cross-Linked CpG Site. The relatively short, interstrand, N^{4}C-ethyl-N^{4}C cross-link forces the alkylated cytidines to adopt a single alternative conformation (B) of the un-cross-linked duplex, due to an unusually large negative propeller twist that minimizes the distance between the exocyclic N4 amines. The X-ray structure reveals that a locally overwound twist and unusual C4′-*exo* sugar pucker at the CpG site also are observed in one conformation of the DNA in the absence of the cross-link, clarifying a previous conjecture based on NMR analysis that the cross-link induced these features. This conformation of the cross-linked deoxyribose interferes with association of a hydrated Ca^{2+} ion, which otherwise is observed in the minor groove of the other un-cross-linked conformation (A). Unique features of the cross-linked CpG site include an increased roll of the base pair that brings together the cytosine amines and optimized hydrogen bonds between the paired cytosine and guanine bases.

Locally, the N4-CX−*CX-N4* bond of the N^{4}C-ethyl-N^{4}C cross-link adopts a staggered, *gauche* conformer, with the CX methylene carbons slightly displaced from the plane of the base. Although the geometry of the Watson−Crick hydrogen bond and lack of hydrogen bond donors near the cross-linked N4 amine are consistent with sp^2-hybridized bond character, the deviation of the CX carbon from the base plane suggests partial sp^3 hybridization. Conventionally, hydrogen atoms bonded to exocyclic amino groups of nucleotide bases are assumed to be coplanar with the base atoms (*21*, *22*), due to conjugation of the lone pair electrons of the nitrogen with the neighboring π-electron cloud of the base. However, ab initio quantum chemical calculations and surveys of hydrogen bonds in small molecule and macromolecular structure databases indicate that, in some cases, the hydrogen atoms bonded to amino groups of nucleoside bases may adopt nonplanar, sp^3-hybridized geometry (*32*−*34*). In the absence of high-resolution neutron diffraction studies (*35*), direct experimental evidence for nonplanar exocyclic amino groups in nucleic acids is minimal. Even in atomic resolution X-ray structures (<1.0 Å resolution), hydrogen atoms are difficult to place due to low atomic scattering factors and generally more dynamic positions. The methylene carbons that replace the hydrogen atoms in the N^{4}C-ethyl-N^{4}C cross-link are clearly observed in the electron density (Figure 1), providing rare experimental evidence for nonplanarity of an exocyclic amino group belonging to a nucleic acid base. This observation reinforces the importance of considering nonplanar amino groups when analyzing the hydrogen bond interactions of nucleic acids with proteins or small molecule ligands.

Comparison with Chemotherapeutic Interstrand DNA Cross-Links and Significance for DNA Repair. The majority of DNA interstrand cross-links induced by antitumor compounds that have been studied structurally thus far are highly distorted, including interstrand cross-links of *cis*-diamminedichloroplatinum (cisplatin, DDP), nitrogen mustards, and psoralen (reviewed in ref *2*). For example, molecular dynamics and electrophoretic mobility experiments show that DNAs cross-linked with the nitrogen mustard mechlorethamine at 5′-GNC-3′ sites are locally distorted and bent by the lesion (*36*). The anticancer compound DDP forms interstrand cross-links between guanines of 5′-GC-3′ sequences that significantly deform the DNA helix (*37*, *38*). Although DDP reacts with the guanine N7 atoms, which are normally located in the major groove of B-form DNA, the

highly distorted DNA conformation places this cross-link in the DNA minor groove and extrudes the cytosines from the dramatically bent and underwound DNA site, as shown by X-ray (*39*) and NMR structural analysis (*40*, *41*), as well as by electrophoretic mobility and chemical footprinting experiments (*42*). Psoralens, which are natural DNA cross-linkers used to treat skin diseases (*43*), intercalate preferentially at AT-rich sites and produce interstrand cross-links between thymidines when irradiated with ultraviolet light (*44*). NMR structures of 4′-hydroxymethyl-4,5′,8-trimethylpsoralen (*45*, *46*) or 4′-aminomethyl-4,5′,8-trimethylpsoralen (*47*) interstrand cross-linked DNA oligonucleotides show that the intercalated and cross-linked site is locally distorted and significantly underwound compared with the canonical B-form. These interstrand cross-linked structures differ remarkably from the largely unaltered, B-form structure of the N^4C-ethyl-N^4C cross-linked CpG site.

Since psoralen interstrand cross-linked DNA is chemically stable and relatively easy to synthesize, many studies on the repair of interstrand cross-links in defined DNA substrates have employed the psoralen interstrand cross-link (*2*). However, in some cases, antitumor compounds result in interstrand cross-links that minimally perturb the DNA structure. For example, the antibiotic mitomycin C (MMC) from *Streptomyces caespitosus* is an important treatment for a variety of cancers (*48*−*50*). MMC forms interstrand cross-links between the exocyclic N2 amines of guanines, which slightly widen the DNA minor groove (*51*), but lacks detectable effect on the overall DNA conformation or bending (*52*). Although interstrand DNA cross-links triggered by MMC are a major cause of cell death, these cross-links occur with low frequency (1 per 20000 base pairs) (*53*, *54*). The UvrABC NER pathway in *E. coli* repairs site-specific interstrand cross-links of a related but more active compound, mitomycin A, particularly in the context of supercoiled plasmid DNA (*55*). However, the low abundance of the MMC interstrand cross-links presents a difficulty for studying the repair mechanism of MMC lesions in defined DNA sites of known sequence. Overall, the X-ray structural analysis presented here and previous NMR experiments (*13*) suggest that N^4C-ethyl-N^4C interstrand cross-linked CpG steps would provide a synthetic model for studying repair of interstrand cross-links of defined sequences in the absence of gross distortions of the DNA helix, such as those produced by MMC. Accordingly, both the alkyl and MMC interstrand cross-links of CpG sites are repaired by the UvrABC pathway in *E. coli* (*13*, *56*).

Remarkably, our high-resolution X-ray structure reveals that the N^4C-ethyl-N^4C interstrand cross-link does not even minimally alter the structure of the un-cross-linked d(C-CAACGTTGG)$_2$ oligonucleotide; rather, one preexisting conformation of the DNA is selectively stabilized by the interstrand cross-link. Moreover, comparison of the N^4C-ethyl-N^4C interstrand cross-linked DNA with the DNA-bound structure of the nucleosome core (*57*) shows that the presence of two methylene carbons deep in the major groove are unlikely to interfere with the DNA contacts of the histone proteins, which are primarily formed with the phosphodiester backbone. Consequently, the N^4C-ethyl-N^4C cross-linked CpG site lacks explicit chemical handles for recognition by DNA repair factors. Nevertheless, the covalent cross-link between the DNA strands would block DNA replication or transcription. Thus, the synthetic, N^4C-ethyl-N^4C interstrand CpG cross-link provides a unique opportunity to study the repair of covalently linked DNA strands in the absence of other prominent features of damaged DNA. Together with studies on the structure and repair of the reversed, N^4C-ethyl-N^4C interstrand GpC cross-link, which significantly disrupts the DNA helix unlike the minimal effects of the CpG cross-link (*13*), this work contributes to a growing arsenal of well-characterized synthetic alkyl interstrand cross-links that can be used to address the detailed structural and mechanistic relationships of DNA repair.

ACKNOWLEDGMENT

We are grateful to L. M. Amzel, D. J. Leahy, and C. Wolberger for advice and generous access to X-ray equipment.

SUPPORTING INFORMATION AVAILABLE

One figure showing the hydrated Ca^{2+} ions bound to the N^4C-ethyl-N^4C cross-linked DNA (Figure S1). This material is available free of charge via the Internet at http://pubs.acs.org.

REFERENCES

1. Scharer, O. D. (2005) DNA interstrand crosslinks: natural and drug-induced DNA adducts that induce unique cellular responses, *ChemBioChem 6*, 27−32.
2. Noll, D. M., Mason, T. M., and Miller, P. S. (2006) Formation and repair of interstrand cross-links in DNA, *Chem. Rev. 106*, 277−301.
3. Niedernhofer, L. J., Daniels, J. S., Rouzer, C. A., Greene, R. E., and Marnett, L. J. (2003) Malondialdehyde, a product of lipid peroxidation, is mutagenic in human cells, *J. Biol. Chem. 278*, 31426−31433.
4. Mathison, B. H., Harman, A. E., and Bogdanffy, M. S. (1997) DNA damage in the nasal passageway: a literature review, *Mutat. Res. 380*, 77−96.
5. Chen, Q., Van der Sluis, P. C., Boulware, D., Hazlehurst, L. A., and Dalton, W. S. (2005) The FA/BRCA pathway is involved in melphalan-induced DNA interstrand cross-link repair and accounts for melphalan resistance in multiple myeloma cells, *Blood 106*, 698−705.
6. Dong, Q., Johnson, S. P., Colvin, O. M., Bullock, N., Kilborn, C., Runyon, G., Sullivan, D. M., Easton, J., Bigner, D. D., Nahta, R., Marks, J., Modrich, P., and Friedman, H. S. (1999) Multiple DNA repair mechanisms and alkylator resistance in the human medulloblastoma cell line D-283 Med (4-HCR), *Cancer Chemother. Pharmacol. 43*, 73−79.
7. Vogel, E. W., Barbin, A., Nivard, M. J., Stack, H. F., Waters, M. D., and Lohman, P. H. (1998) Heritable and cancer risks of exposures to anticancer drugs: inter-species comparisons of covalent deoxyribonucleic acid-binding agents, *Mutat. Res. 400*, 509−540.
8. O'Connor, P. M., and Kohn, K. W. (1990) Comparative pharmacokinetics of DNA lesion formation and removal following treatment of L1210 cells with nitrogen mustards, *Cancer Commun. 2*, 387−394.
9. Noronha, A. M., Wilds, C. J., and Miller, P. S. (2002) N(4)C-alkyl-N(4)C cross-linked DNA: bending deformations in duplexes that contain a -CNG- interstrand cross-link, *Biochemistry 41*, 8605−8612.
10. Noll, D. M., Noronha, A. M., and Miller, P. S. (2001) Synthesis and characterization of DNA duplexes containing an N(4)C-ethyl-N(4)C interstrand cross-link, *J. Am. Chem. Soc. 123*, 3405−3411.
11. Noronha, A. M., Noll, D. M., and Miller, P. S. (2001) Syntheses of DNA duplexes containing a C-C interstrand cross-link, *Nucleosides, Nucleotides Nucleic Acids 20*, 1303−1307.
12. Noronha, A. M., Noll, D. M., Wilds, C. J., and Miller, P. S. (2002) N(4)C-ethyl-N(4)C cross-linked DNA: synthesis and characteriza-

tion of duplexes with interstrand cross-links of different orientations, *Biochemistry 41*, 760−771.
13. Noll, D. M., Webba da Silva, M., Noronha, A. M., Wilds, C. J., Colvin, O. M., Gamcsik, M. P., and Miller, P. S. (2005) Structure, flexibility, and repair of two different orientations of the same alkyl interstrand DNA cross-link, *Biochemistry 44*, 6764−6775.
14. Chiu, T. K., and Dickerson, R. E. (2000) 1 Å crystal structures of B-DNA reveal sequence-specific binding and groove-specific bending of DNA by magnesium and calcium, *J. Mol. Biol. 301*, 915−945.
15. Jones, T. A., Zou, J. Y., Cowan, S. W., and Kjeldgaard (1991) Improved methods for building protein models in electron density maps and the location of errors in these models, *Acta Crystallogr. A 47* (Part 2), 110−119.
16. Kleygwegt, G. J., Zou, J. Y., Kjeldgaard, M., and Jones, T. A. (2001) Around O, in *International Tables for Crystallography, Volume F. Crystallography of Biological Macromolecules* (Rossmann, M. G., and Arnold, E., Eds.) pp 353−356, 366−367, Kluwer Academic Publishers, Dordrecht, The Netherlands.
17. Brunger, A. T., Adams, P. D., Clore, G. M., DeLano, W. L., Gros, P., Grosse-Kunstleve, R. W., Jiang, J. S., Kuszewski, J., Nilges, M., Pannu, N. S., Read, R. J., Rice, L. M., Simonson, T., and Warren, G. L. (1998) Crystallography & NMR system: A new software suite for macromolecular structure determination, *Acta Crystallog.r D 54* (Part 5), 905−921.
18. Read, R. (1986) Improved Fourier coefficients for maps using phases from partial structures with errors, *Acta Crystallogr. A 42*, 140−149.
19. Lavery, R., and Sklenar, H. (1988) The definition of generalized helicoidal parameters and of axis curvature for irregular nucleic acids, *J. Biomol. Struct. Dyn. 6*, 63−91.
20. Saenger, W. (1984) *Principles of Nucleic Acid Structure*, Springer-Verlag, New York.
21. Cornell, W. D., Cieplak, P., Bayly, C. I., Gould, I. R., Merz, K. M. J., Ferguson, D. M., Spellmeyer, D. C., Fox, T., Caldwell, J. W., and Kollman, P. A. (1995) A second generation force field for simulation of proteins, nucleic acids, and organic molecules, *J. Am. Chem. Soc. 117*, 5179−5197.
22. Mackerell, A. D., Wiorkiewiczkuczera, J., and Karplus, M. (1995) An all-atom empirical energy function for the simulation of nucleic acids, *J. Am. Chem. Soc. 117*, 11946−11975.
23. Collaborative Computational Project (1994) The CCP4 Suite: Programs for Protein Crystallography, *Acta Crystallogr. D50*, 760−763.
24. Jeffrey, G. A. (1997) *An Introduction to Hydrogen Bonding*, Oxford University Press, New York.
25. Garbuzynskiy, S. O., Melnik, B. S., Lobanov, M. Y., Finkelstein, A. V., and Galzitskaya, O. V. (2005) Comparison of X-ray and NMR structures: is there a systematic difference in residue contacts between X-ray- and NMR-resolved protein structures?, *Proteins 60*, 139−147.
26. Prive, G. G., Yanagi, K., and Dickerson, R. E. (1991) Structure of the B-DNA decamer C-C-A-A-C-G-T-T-G-G and comparison with isomorphous decamers C-C-A-A-G-A-T-T-G-G and C-C-A-G-G-C-C-T-G-G, *J. Mol. Biol. 217*, 177−199.
27. Gold, B., Marky, L. M., Stone, M. P., and Williams, L. D. (2006) A review of the role of the sequence-dependent electrostatic landscape in DNA alkylation patterns, *Chem. Res. Toxicol. 19*, 1402−1414.
28. Minasov, G., Tereshko, V., and Egli, M. (1999) Atomic-resolution crystal structures of B-DNA reveal specific influences of divalent metal ions on conformation and packing, *J. Mol. Biol. 291*, 83−99.
29. Katz, A. K., Glusker, J. P., Beebe, S. A., and Bock, C. W. (1996) Calcium ion coodination: A comparison with that of beryllium, magnesium, and zinc, *J. Am. Chem. Soc. 118*, 5752−5763.
30. Vitali, J., Ding, J., Jiang, J., Zhang, Y., Krainer, A. R., and Xu, R. M. (2002) Correlated alternative side chain conformations in the RNA-recognition motif of heterogeneous nuclear ribonucleoprotein A1, *Nucleic Acids Res. 30*, 1531−1538.
31. Thickman, K. R., Sickmier, E. A., and Kielkopf, C. L. (2006) Alternative conformations at the RNA binding surface of the N-terminal U2AF65 RNA recognition motif, *J. Mol. Biol.* (in press) (doi: 10.1016/j.jmb.2006.11.077).
32. Mukherjee, S., Majumdar, S., and Bhattacharyya, D. (2005) Role of hydrogen bonds in protein-DNA recognition: Effect of nonplanar amino groups, *J. Phys. Chem. B 109*, 10484−10492.
33. Luisi, B., Orozco, M., Sponer, J., Luque, F. J., and Shakked, Z. (1998) On the potential role of the amino nitrogen atom as a hydrogen bond acceptor in macromolecules, *J. Mol. Biol. 279*, 1123−1136.
34. Bludsky, O., Sponer, J., Leszczynski, J., Spirka, V., and Hobza, P. (1996) Amino groups in nucleic acid bases, aniline, aminopyridines, and aminotriazine are nonplanar: Results of correlated *ab initio* quantum chemical calculations and anharmonic analysis of the aniline inversion motion, *J. Chem. Phys. 105*, 11042−11050.
35. Arai, S., Chatake, T., Ohhara, T., Kurihara, K., Tanaka, I., Suzuki, N., Fujimoto, Z., Mizuno, H., and Niimura, N. (2005) Complicated water orientations in the minor groove of the B-DNA decamer $d(CCATTAATGG)_2$ observed by neutron diffraction measurements, *Nucleic Acids Res. 33*, 3017−3024.
36. Rink, S. M., and Hopkins, P. B. (1995) A mechlorethamine-induced DNA interstrand cross-link bends duplex DNA, *Biochemistry 34*, 1439−1445.
37. Cohen, S. M., and Lippard, S. J. (2001) Cisplatin: from DNA damage to cancer chemotherapy, *Prog. Nucleic Acid Res. Mol. Biol. 67*, 93−130.
38. Kartalou, M., and Essigmann, J. M. (2001) Recognition of cisplatin adducts by cellular proteins, *Mutat. Res. 478*, 1−21.
39. Coste, F., Malinge, J. M., Serre, L., Shepard, W., Roth, M., Leng, M., and Zelwer, C. (1999) Crystal structure of a double-stranded DNA containing a cisplatin interstrand cross-link at 1.63 Å resolution: hydration at the platinated site, *Nucleic Acids Res. 27*, 1837−1846.
40. Paquet, F., Perez, C., Leng, M., Lancelot, G., and Malinge, J. M. (1996) NMR solution structure of a DNA decamer containing an interstrand cross-link of the antitumor drug cis-diamminedichloroplatinum (II), *J. Biomol. Struct. Dyn. 14*, 67−77.
41. Huang, H., Zhu, L., Reid, B. R., Drobny, G. P., and Hopkins, P. B. (1995) Solution structure of a cisplatin-induced DNA interstrand cross-link, *Science 270*, 1842−1845.
42. Malinge, J. M., Perez, C., and Leng, M. (1994) Base sequence-independent distorsions induced by interstrand cross-links in cis-diamminedichloroplatinum (II)-modified DNA, *Nucleic Acids Res. 22*, 3834−3839.
43. Brenner, M., Herzinger, T., Berking, C., Plewig, G., and Degitz, K. (2005) Phototherapy and photochemotherapy of sclerosing skin diseases, *Photodermatol. Photoimmunol. Photomed. 21*, 157−165.
44. Hearst, J. E. (1981) Psoralen photochemistry, *Annu. Rev. Biophys. Bioeng. 10*, 69−86.
45. Spielmann, H. P., Dwyer, T. J., Sastry, S. S., Hearst, J. E., and Wemmer, D. E. (1995) DNA structural reorganization upon conversion of a psoralen furan-side monoadduct to an interstrand cross-link: implications for DNA repair, *Proc. Natl. Acad. Sci. U.S.A. 92*, 2345−2349.
46. Spielmann, H. P., Dwyer, T. J., Hearst, J. E., and Wemmer, D. E. (1995) Solution structures of psoralen monoadducted and cross-linked DNA oligomers by NMR spectroscopy and restrained molecular dynamics, *Biochemistry 34*, 12937−12953.
47. Hwang, G. S., Kim, J. K., and Choi, B. S. (1996) The solution structure of a psoralen cross-linked DNA duplex by NMR and relaxation matrix refinement, *Biochem. Biophys. Res. Commun. 219*, 191−197.
48. Chalasani, R., Giblin, M., and Conway, R. M. (2006) Role of topical chemotherapy for primary acquired melanosis and malignant melanoma of the conjunctiva and cornea: review of the evidence and recommendations for treatment, *Clin. Exp. Ophthalmol. 34*, 708−714.
49. Eifel, P. J. (2006) Chemoradiotherapy in the treatment of cervical cancer, *Semin. Radiat. Oncol. 16*, 177−185.
50. Bolenz, C., Cao, Y., Arancibia, M. F., Trojan, L., Alken, P., and Michel, M. S. (2006) Intravesical mitomycin C for superficial transitional cell carcinoma, *Expert Rev. Anticancer Ther. 6*, 1273−1282.
51. Norman, D., Live, D., Sastry, M., Lipman, R., Hingerty, B. E., Tomasz, M., Broyde, S., and Patel, D. J. (1990) NMR and computational characterization of mitomycin cross-linked to adjacent deoxyguanosines in the minor groove of the d(T-A-C-G-T-A)d(T-A-C-G-T-A) duplex, *Biochemistry 29*, 2861−2875.
52. Rink, S. M., Lipman, R., Alley, S. C., Hopkins, P. B., and Tomasz, M. (1996) Bending of DNA by the mitomycin C-induced, GpG intrastrand cross-link, *Chem. Res. Toxicol. 9*, 382−389.

53. Iyer, V. N., and Szybalski, W. (1964) Mitomycins and porfiromycin: chemical mechanism of activation and cross-linking of DNA, *Science 145*, 55−58.
54. Iyer, V. N., and Szybalski, W. (1963) A molecular mechanism of mitomycin action: linking of complementary DNA strands, *Proc. Natl. Acad. Sci. U.S.A. 50*, 355−362.
55. Pu, W. T., Kahn, R., Munn, M. M., and Rupp, W. D. (1989) UvrABC incision of N-methylmitomycin A-DNA monoadducts and cross-links, *J. Biol. Chem. 264*, 20697−20704.
56. Vidal, L. S., Santos, L. B., Lage, C., and Leitao, A. C. (2006) Enhanced sensitivity of *Escherichia coli* uvrB mutants to mitomycin C points to a UV-C distinct repair for DNA adducts, *Chem. Res. Toxicol. 19*, 1351−1356.
57. Luger, K., Mader, A. W., Richmond, R. K., Sargent, D. F., and Richmond, T. J. (1997) Crystal structure of the nucleosome core particle at 2.8 Å resolution, *Nature 389*, 251−260.

BI700109R